The NF-#B Genomic Landscape in Lymphoblastoid B Cells

Citation: Zhao, Bo, Luis A. Barrera, Ina Ersing, Bradford Willox, Stefanie C.S. Schmidt, Hannah Greenfeld, Hufeng Zhou, et al. "The NF-κB Genomic Landscape in Lymphoblastoid B Cells." Cell Reports 8, no. 5 (September 2014): 1595–1606.

As Published: http://dx.doi.org/10.1016/j.celrep.2014.07.037

Publisher: Elsevier

Persistent URL: http://hdl.handle.net/1721.1/100778

Version: Final published version: final published article, as it appeared in a journal, conference proceedings, or other formally published context

Cell Reports
Resource

The NF-κB Genomic Landscape in Lymphoblastoid B Cells

Bo Zhao,[1,2,9] Luis A. Barrera,[3,4,5,6,7,9] Ina Ersing,[1,2] Bradford Willox,[1] Stefanie C.S. Schmidt,[1,2] Hannah Greenfeld,[1] Hufeng Zhou,[1,2] Sarah B. Mollo,[1,2] Tommy T. Shi,[1] Kaoru Takasaki,[1] Sizun Jiang,[1,2] Ellen Cahir-McFarland,[1] Manolis Kellis,[7] Martha L. Bulyk,[3,4,5,6,8,10,*] Elliott Kieff,[1,2,10] and Benjamin E. Gewurz[1,2,10,*]
[1]Division of Infectious Disease, Department of Medicine, Brigham and Women's Hospital, Boston, MA 02115, USA
[2]Department of Microbiology and Immunobiology, Harvard Medical School, Boston, MA 02115, USA
[3]Division of Genetics, Department of Medicine, Brigham and Women's Hospital, Boston, MA 02115, USA
[4]Harvard Medical School, Boston, MA 02115, USA
[5]Committee on Higher Degrees in Biophysics, Harvard University, Cambridge, MA 02138, USA
[6]Harvard-MIT Division of Health Sciences and Technology, Harvard Medical School, Boston, MA 02115, USA
[7]Computer Science and Artificial Intelligence Laboratory, Massachusetts Institute of Technology, Cambridge, MA 02139, USA
[8]Department of Pathology, Brigham and Women's Hospital, Boston, MA 02115, USA
[9]Co-first author
[10]Co-senior author
*Correspondence: mlbulyk@receptor.med.harvard.edu (M.L.B.), bgewurz@partners.org (B.E.G.)
http://dx.doi.org/10.1016/j.celrep.2014.07.037

SUMMARY

The nuclear factor κB (NF-κB) subunits RelA, RelB, cRel, p50, and p52 are each critical for B cell development and function. To systematically characterize their responses to canonical and noncanonical NF-κB pathway activity, we performed chromatin immunoprecipitation followed by high-throughput DNA sequencing (ChIP-seq) analysis in lymphoblastoid B cell lines (LCLs). We found a complex NF-κB-binding landscape, which did not readily reflect the two NF-κB pathway paradigms. Instead, 10 subunit-binding patterns were observed at promoters and 11 at enhancers. Nearly one-third of NF-κB-binding sites lacked κB motifs and were instead enriched for alternative motifs. The oncogenic forkhead box protein FOXM1 co-occupied nearly half of NF-κB-binding sites and was identified in protein complexes with NF-κB on DNA. FOXM1 knockdown decreased NF-κB target gene expression and ultimately induced apoptosis, highlighting FOXM1 as a synthetic lethal target in B cell malignancy. These studies provide a resource for understanding mechanisms that underlie NF-κB nuclear activity and highlight opportunities for selective NF-κB blockade.

INTRODUCTION

The nuclear factor κB (NF-κB) is a family of dimeric transcription factors (TFs) that mediate differentiation, development, proliferation, and survival (Hayden and Ghosh, 2012). NF-κB is a principal component of the body's defense against infection and is critically important for most immune and inflammatory responses. Yet, NF-κB hyperactivation contributes to inflammatory disorders and cancer, in particular B cell malignancies (Ben-Neriah and Karin, 2011; Lim et al., 2012). Despite progress in understanding cytosolic pathways that activate NF-κB TFs, comparatively little is known about the mechanisms that govern nuclear NF-κB function (Natoli, 2009; Smale, 2011; Wan and Lenardo, 2010).

Microbes nonetheless use NF-κB to enable their replication and spread. Oncogenic viruses encode factors that constitutively activate NF-κB, including Epstein-Barr virus (EBV), Kaposi's sarcoma-associated herpesvirus, human T cell leukemia virus, hepatitis B, and hepatitis C (Rahman and McFadden, 2011). Constitutive NF-κB activation also contributes to the pathogenesis of numerous human cancers, in particular B cell lymphomas (Ben-Neriah and Karin, 2011; Lim et al., 2012). However, the genome-wide effects of constitutive NF-κB activation on NF-κB TF binding have not been defined.

Mammalian genomes encode five NF-κB subunits: p105/p50, p100/p52, RelA (p65), RelB, and cRel. Each has an N-terminal Rel homology domain that mediates sequence-specific binding to DNA κB sites (Hayden and Ghosh, 2012). RelA, RelB, and cRel also have C-terminal transcription activation domains. NF-κB dimers can further induce or suppress target gene expression through cofactor recruitment. Inhibitor of NF-κB (IκB) proteins retain NF-κB dimers in the cytosol, with the exception of p50 homodimers, which are constitutively nuclear (Hayden and Ghosh, 2012).

Two NF-κB pathways trigger NF-κB activity by inducing IκB degradation and NF-κB nuclear translocation (Bonizzi and Karin, 2004). The canonical pathway responds to proinflammatory signals and is essential for rapid immune responses. The canonical pathway triggers IκBα degradation, which enables RelA and cRel-containing complexes to translocate to the nucleus, including RelA:p50, cRel:p50, RelA:RelA, and cRel:cRel

dimers. The noncanonical NF-κB pathway promotes secondary lymphoid organogenesis, B cell development, and survival (Sun, 2011). The noncanonical pathway triggers processing of p100 to p52, which enables the p52-containing complexes RelB:p52, p52:p52, and p50:p52 to enter the nucleus.

When both pathways are active in B cells, up to 14 distinct NF-κB dimers form, including canonical/noncanonical hybrids such as RelA:p52 (Shih et al., 2011). Murine genetic studies indicate that each NF-κB subunit, and perhaps each dimer, has unique functions in B cell development and activation (Gerondakis et al., 2006). The generation and maintenance of mature B cells require both canonical and noncanonical NF-κB pathway activity (Kaileh and Sen, 2012). CD40-mediated activation of both pathways is required for B cell responses such as homotypic aggregation, which requires both cRel and p52 (Zarnegar et al., 2004). Yet, the extent of intrinsic NF-κB dimer-binding preference for its target sites in vivo and the mechanisms that establish dimer-specific binding are not understood well. Likewise, little is known about the extent to which target genes are regulated independently, or jointly, by the canonical and noncanonical pathways.

κB sites in mammalian genomes vary widely from the consensus sequence 5′-GGGRNYYYCC-3′ (where R is a purine, Y is a pyrimidine, and N is any nucleotide). Moreover, a single base pair difference in a κB site can induce distinct NF-κB dimer conformations and affect coactivator requirements (Leung et al., 2004). The extent to which NF-κB family members differentially recruit TFs to κB sites remains to be examined in vivo. Likewise, NF-κB recruitment by other sequence-specific TFs to non-κB DNA sites has not been extensively investigated.

To date, genome-scale analyses of NF-κB binding by chromatin immunoprecipitation (ChIP)-based methods have generally been limited to RelA (Heinz et al., 2013; Jin et al., 2013; Kasowski et al., 2010; Lim et al., 2007; Martone et al., 2003). Where multiple subunits were studied, cells were stimulated by Toll-like receptor agonists that preferentially activate the canonical NF-κB pathway (Garber et al., 2012; Schreiber et al., 2006). In B cells, only RelA has been studied systematically (Kasowski et al., 2010).

To systematically investigate how NF-κB TFs recognize in vivo targets, we performed chromatin immunoprecipitation followed by deep-sequencing (ChIP-seq) analysis of all five NF-κB subunits in the EBV-transformed lymphoblastoid B cell line (LCL) GM12878, where the EBV-encoded membrane protein LMP1 mimics CD40 to constitutively activate the canonical and noncanonical NF-κB pathways (Longnecker et al., 2013). GM12878 has a relatively normal karyotype, is one of three ENCODE (Encyclopedia of DNA Elements) project Tier 1 cell lines, and is an original HapMap cell line used in many genetic studies. We identified a complex NF-κB-binding landscape, with distinct NF-κB subunit-binding patterns (SBPs) at LCL promoters and enhancers, and with frequent recruitment of NF-κB to DNA sites that lack κB motifs. Numerous B cell TFs co-occupied LCL NF-κB sites, including the Forkhead box protein FOXM1. FOXM1 was present at nearly half of all LCL NF-κB sites and was recruited to NF-κB complexes on DNA. Collectively, our results provide insights into B cell nuclear NF-κB regulation, including CD40-stimulated germinal center B cells and lymphomas with constitutive NF-κB activity.

RESULTS

Genome-wide NF-κB Subunit DNA Binding in Lymphoblastoid B Cells

ChIP-seq was used to assess NF-κB subunit DNA binding in GM12878 cells. Validated anti-RelA, anti-RelB, anti-cRel, and anti-p50 antibodies were used, each of which has been shown to be specific by western blot and ChIP (Baek et al., 2002; Huang et al., 2000; Liu and Beller, 2003; Martone et al., 2003; Nissen and Yamamoto, 2000; Rodriguez et al., 1999; Saccani et al., 2003; Wang et al., 1997; Yamazaki and Kurosaki, 2003) and by a ChIP-microarray analysis of NF-κB promoter occupancy in lipopolysaccharide (LPS)-stimulated monocytes (Schreiber et al., 2006). Anti-p52 antibody specificity was validated by immunoprecipitation (Figure S1).

Using highly concordant biological replicates (Figure S2; Table S1), we identified 20,067 RelA, 16,617 RelB, 6,765 cRel, 4,298 p50, and 10,814 p52 peaks, with an irreproducible discovery rate (IDR) of <0.01 (Landt et al., 2012), significantly expanding the known number of B cell NF-κB-binding sites. Data sets for each NF-κB subunit exceeded ENCODE project quality control standards (Landt et al., 2012), and our sequencing depth was therefore more than sufficient to capture biologically meaningful binding (Figure S2; Table S1; Supplemental Experimental Procedures). For instance, the ratio of sequencing tag abundance inside versus outside of peaks, a standard measure of noise in ChIP-seq experiments, was 3.1% for RelA, 4.6% for RelB, 0.9% for cRel, 2.2% for p50, and 2.8% for p52. Thus, differences across experiments were moderate. Furthermore, we took multiple steps to eliminate differences that arose from sequence depth effects, including normalization of ChIP signals across experiments (Ye et al., 2011) (Supplemental Experimental Procedures). Where an NF-κB-binding site was identified for any subunit, we cross-compared raw signals for all five subunits at that site, rather than restricting analysis to only the called peaks. Robust peaks for all NF-κB subunits were evident at κB sites at many well-characterized B cell κB target genes, including the *BCL2* locus (Figure 1A).

Using validated GM12878 chromatin state annotations based on histone modifications (Ernst et al., 2011), we found NF-κB predominantly (73%) at active enhancers, as characterized by H3K4me1 and H3K27ac marks (Figure 1B). For example, the dominant *BCL2* NF-κB peaks localized to an enhancer (Figure 1A). Nonetheless, in comparison with other NF-κB subunits, a higher proportion of cRel peaks occurred at active promoters (~40% of all cRel peaks), as defined by H3K4me3 and H3K9ac marks. At 24.7% of cRel peaks, cRel was the dominant NF-κB subunit, putatively binding as a homodimer. By contrast, only ~15% of mapped RelB peaks localized to active promoters. NF-κB-binding site motifs derived de novo from the ChIP-seq data were similar to each other, with the cRel motif showing increased degeneracy in its 5′ half-site and p50 exhibiting a longer motif (Figure 1C).

Patterns of NF-κB Subunit Cobinding

A rich NF-κB dimer milieu was present in LCL nuclei (Figure S1). For instance, RelA and cRel bound to similar amounts of p50

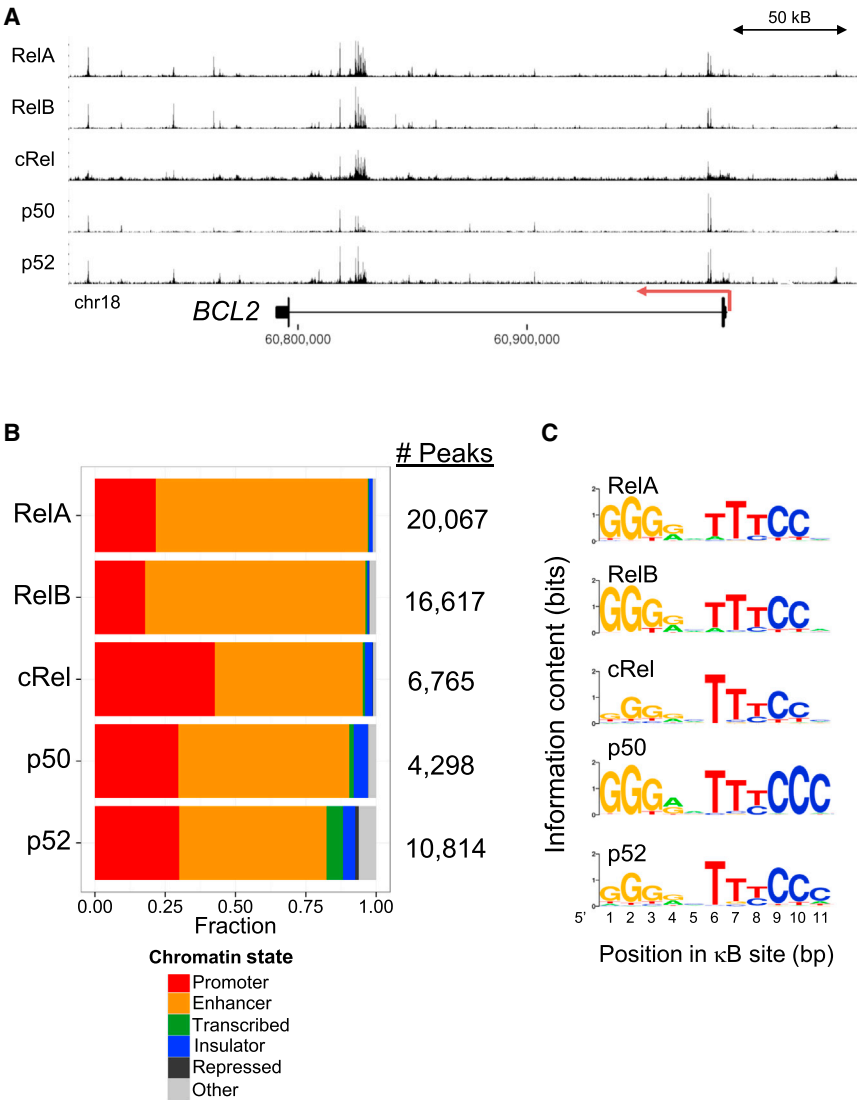

Figure 1. NF-κB Subunit Genome-wide Distribution and Consensus Motif

(A) NF-κB subunit ChIP-seq signals at the *BCL2* locus. The y axis is scaled between 0 and 20 times the median signal value of the surrounding 100 kb. chr18, chromosome 18.

(B) Genome-wide NF-κB subunit distribution across chromatin states, as defined by GM12878 histone modifications, CTCF, and Pol2 occupancy. Each horizontal bar shows the fraction of NF-κB subunit peaks that were assigned to each chromatin state. The total number of NF-κB subunit peaks is shown to the right of each bar.

(C) Consensus de novo motif for each NF-κB subunit.

and p52, and at a lower level, to each other. By contrast, RelB preferentially associated with p52, to a lower level with p50, and to a substantially lower level with RelA. Both p50 and p52 associate with all NF-κB subunits (Figure S1). κB sites in theory could be bound by a single NF-κB dimer or could be accessed by distinct NF-κB dimer combinations in equilibrium with one another.

To identify NF-κB SBPs, we applied k-means clustering to the ChIP-seq data. We found 10 distinct SBPs at LCL promoters and 11 at enhancers (Figures 2A and 2B). SBPs with binding by multiple NF-κB subunits likely reflected NF-κB dimer exchange at these sites, rather than simultaneous binding by distinct NF-κB dimers to a single site. In support of the specificity of the antibodies used and despite the RelA data set having the highest number of peaks, clusters with predominant binding by each of the NF-κB subunits were observed at promoters and enhancers, except for RelA. To minimize the possibility that SBPs arose from differences in peak number alone, we generated k-means-clustered heatmaps using only the top-scoring 4,000 peaks for each subunit. Even when using an equal number of peaks for each subunit, very similar SBPs were again observed, suggesting that SBPs do not arise from differences in antibody sensitivity alone (Figure S3A).

Intriguingly, some SBPs were evident at both promoters and enhancers, whereas others were unique to either. For example, cluster P10 promoters, but no enhancer clusters, were occupied by all NF-κB subunits except cRel. Combinations of distinct SBPs were observed at several key NF-κB target genes, such as at the seven NF-κB ChIP-seq peaks near the highly LMP1-induced target gene *TRAF1* (Figure 2C).

We reasoned that ChIP-seq analysis of the five NF-κB subunits in GM12878 might identify target genes unique to either pathway. Indeed, we found SBPs with predominant cRel (clusters P5 and E10) or p52 (clusters P7 and E11) binding, indicative of canonical versus noncanonical activity, respectively (Figures 2A and 2B). Strikingly, most observed SBPs were not readily explained by subunits that are activated by just one pathway. Rather, they were hybrids that resulted from activation of both pathways. For example, cluster E1 and P1 genomic regions were highly occupied by all five NF-κB subunits and were therefore targeted by subunits activated by both NF-κB pathways. Similarly, RelA, RelB, cRel, and p52 were present at clusters P3, E2, and E6. The abundance of RelA, RelB, and cRel heterodimers with p50 and with p52 in LCL nuclei (Figure S1), as well as NF-κB homodimers, likely contributed to these patterns. Although p50- and p52-containing heterodimers are prototypical canonical and noncanonical pathway dimers, respectively, RelA, RelB, and/or cRel predominated at clusters P5, P9, E4, E7, E8, and E10. These results indicate that both NF-κB pathways contribute to the activation of many LMP1 target genes in LCLs.

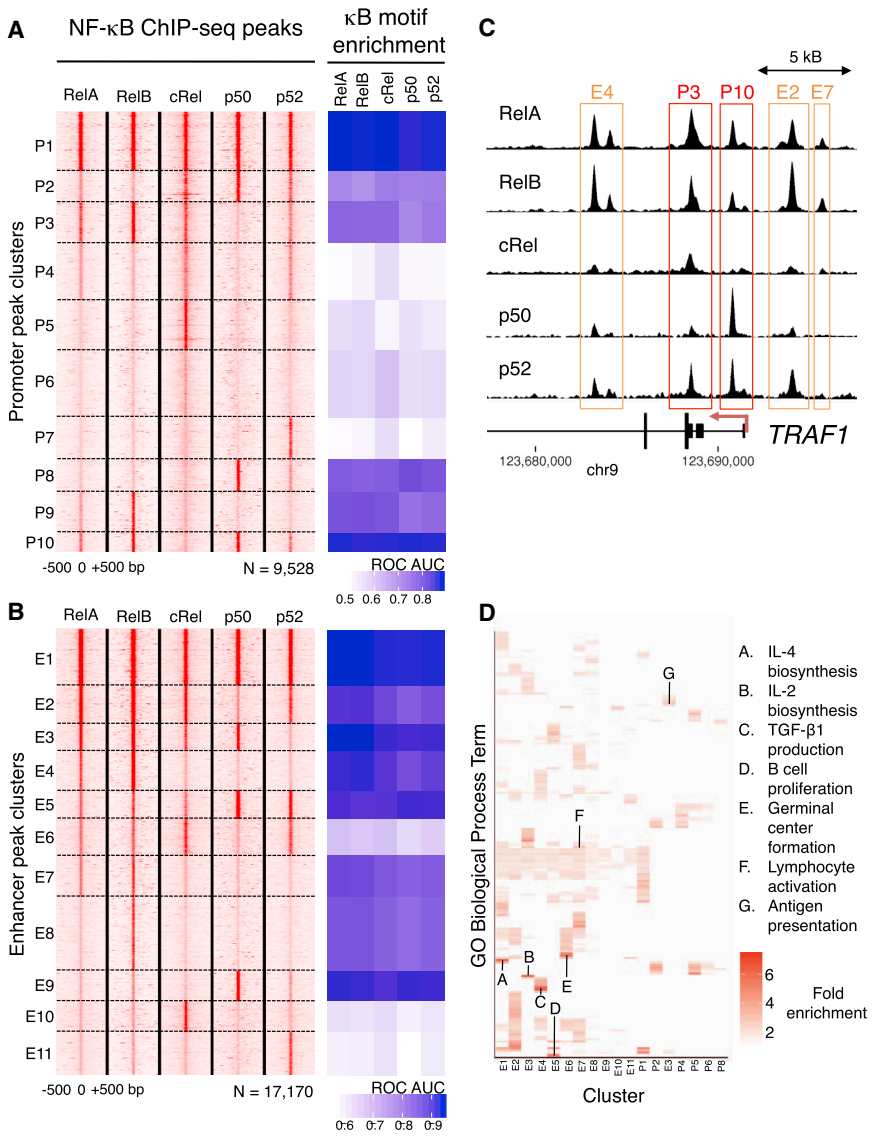

Figure 2. NF-κB Subunit-Binding Profiles

(A and B) A total of 10 promoter (A) and 11 enhancer (B) peak clusters with distinct NF-κB subunit-binding profiles were identified by k-means clustering of ChIP-seq signals at regions bound by at least 1 subunit. Red values indicate higher ChIP-seq signal intensity. The total number of promoter versus enhancer NF-κB-binding sites is shown at the lower right. The heatmap to the right of the peak clusters displays the extent of consensus de novo NF-κB subunit motif enrichment in each cluster. See also Figure S3A.

(C) NF-κB subunit ChIP-seq signals at the TRAF1 locus illustrate the co-occurrence of multiple SBPs at an NF-κB target gene. Red boxes enclose promoter-associated peaks, and orange boxes enclose enhancer-associated peaks. chr9, chromosome 9.

(D) Gene set enrichment analysis of NF-κB clusters using GO Biological Process (BP) terms, as determined by GREAT analysis. Each row corresponds to a unique GO BP term with a false discovery rate (FDR) of <0.01. A subset of highly enriched terms is highlighted. IL-4, interleukin-4; TGF-β1, transforming growth factor β1.

See also Table S2.

SBPs Are Associated with Unique Biological Processes

To investigate whether NF-κB binding at promoters versus enhancers might correspond to different LCL biological functions, we evaluated each cluster for enrichment of Gene Ontology (GO) annotation terms. We used GREAT (McLean et al., 2010) analysis to assign ChIP-seq peaks to their putative target genes, mainly by proximity. Most clusters were enriched for distinct GO Biological Process terms and mouse knockout phenotypes (Figure 2D; Table S2), consistent with the hypothesis that different SBPs have distinct roles in NF-κB responses. Because the formation of many SBPs requires both NF-κB pathways to be active, this result has relevance for the observation that CD40-mediated canonical and noncanonical pathway activation engenders phenotypes that activation of either pathway alone does not produce (Zarnegar et al., 2004). Strikingly, we obtained a larger number of significantly enriched GO terms at enhancers than at promoters and observed that promoter clusters were typically enriched for "housekeeping" functions, whereas enhancer clusters were often enriched for B cell-specific functions.

An 11 bp κB Motif with 3′ Cytosine Is Enriched in All Clusters with p50 Occupancy

The canonical κB motif is 10 bp long, although in vitro studies have found that different NF-κB dimers prefer sites that are 9–12 bp (Siggers et al., 2012). The p50 homodimer recognizes an 11 bp κB motif and makes base-specific contacts with cytosine at position 11 (Chen and Ghosh, 1999; Müller et al., 1995). LCL ChIP-bound p50-binding sites were highly enriched for an 11 bp κB motif ending in cytosine, providing genome-wide confirmation of the importance of this p50 recruitment motif (Figure 3A). The extent of 11 bp enrichment at in vivo p50-binding sites was unexpected because p50 homodimers and, to a lesser extent, p50 heterodimers exhibited moderate preference for this motif in vitro (Siggers et al., 2012). Because the 11 bp κB motif was highly enriched in all clusters with high p50 ChIP signal, and because LCLs contain abundant p50 heterodimers (Figure S1), our results suggest that p50 heterodimers also prefer the 11 bp site (Figures 3A and S3). The 3′ cytosine in p50-bound sites was evolutionarily conserved across 33 mammalian species (Figures 3C and S3), supporting its importance. The fifth, largely degenerate, base pair in κB motif instances was also frequently conserved, consistent with this position influencing cofactor requirements (Leung et al., 2004).

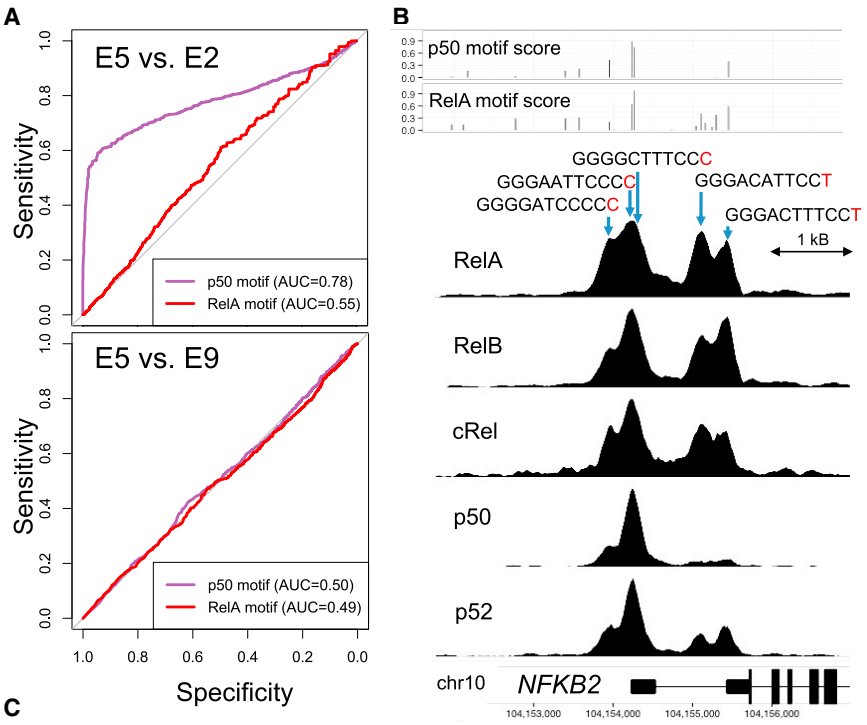

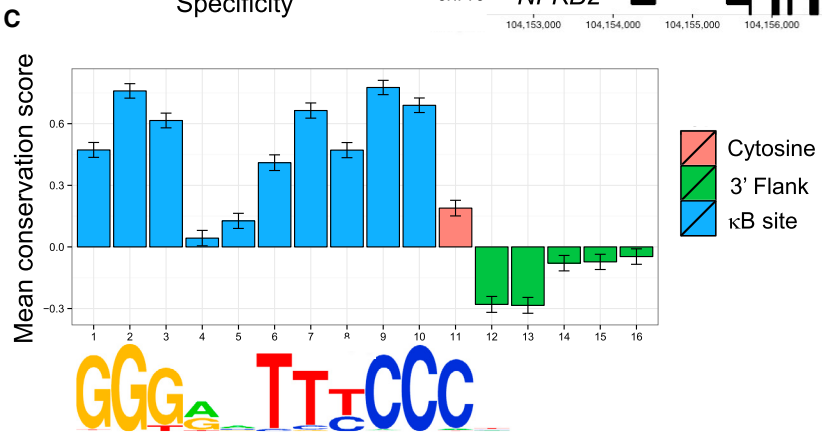

Figure 3. Effect of an 11 bp Motif with a 3′ Cytosine on p50 Recruitment to NF-κB Sites

(A) ROC curves show that the p50 motif 11th bp cytosine predicts p50 ChIP occupancy with high specificity. In the comparisons shown, peaks from clusters E5 and E2 (top; differential p50 binding) and E5 and E9 (bottom; both bound by p50) are compared. The maximum p50, but not RelA, motif match score for each sequence predicts whether peaks belong to E5 (defined as a positive) or to E2 (negative). Meanwhile, neither motif has predictive power when comparing the p50-bound clusters E5 and E9. See also Figures S3B–S3D.

(B) p50 signals are significantly higher at *NFKB2* locus-binding sites that contain the 11 bp motif. Other NF-κB subunits bind more uniformly. Motif match scores are scaled from a minimum match threshold of 0.0 to a maximum of 1.0. chr10, chromosome 10.

(C) The functional importance of the p50-preferred 11 bp κB site 3′ cytosine is supported by its evolutionary conservation across 33 mammalian species. Each bar shows the mean GERP++ score (higher values indicate more evolutionary constraint) at various positions of κB motif instances. Error bars indicate 1 SEM. See also Figure S3E.

Effect of κB Motifs on Subunit Binding

We investigated the extent to which specific κB motif sequences determined each SBP. We compared κB sites at ChIP peaks in each cluster with protein-binding microarray (PBM) data, which provide binding preferences for specific NF-κB (Siggers et al., 2012). We calculated the area under the (AUC) receiver operating characteristic (ROC) curve as a measure of motif or 12-mer enrichment in each cluster. The enrichment values obtained using ChIP-derived de novo motifs (Figures 2A and 2B) were generally similar to those obtained using PBM-derived 12-mer data (Figure S3F). Unexpectedly, most NF-κB binding in GM12878 cells occurred via higher-affinity, traditional κB sites. Aside from the discriminatory power afforded by the 3′ cytosine in the 11 bp κB motif, the κB motif did not vary greatly across clusters, suggesting that other mechanisms were responsible for establishing specific NF-κB-binding patterns.

NF-κB Recruitment to DNA Sites that Lack a κB Motif

Nearly one-third of LCL NF-κB subunit-bound active promoters and enhancers lacked a κB motif. Interestingly, four promoter (clusters P4–P7) and three enhancer clusters (clusters E6, E10, and E11) were not highly enriched for a κB motif, suggesting alternative mechanisms for NF-κB recruitment to these sites (Figures 2A, 2B, and S3F). Although NF-κB recruitment to DNA regions that lack κB sites has been observed previously, alternative motifs that directly or indirectly recruit NF-κB to these sites had not been identified. Using de novo motif discovery, we identified four alternative motifs that were associated with specific combinations of NF-κB subunit binding in LCLs and that may participate in NF-κB recruitment to these sites.

First, we asked how cRel might selectively be recruited to promoters in the absence of κB motifs (cluster P5), and found significant enrichment of E box motifs (AUC, 0.61; $p = 1.66 \times 10^{-18}$) (Figure 4). Indeed, the basic-helix-loop-helix (bHLH) TFs USF1 and USF2, which recognize E box motifs, co-occupied 40.2% and 39.3% of GM12878 cluster P5 regions, respectively (Figures 4 and 5). Our results support a model in which bHLH factors recruit cRel homodimers to LCL E box sites.

p52 was selectively recruited to genomic regions belonging to clusters P7 and E11. De novo motif analyses identified a composite ETS (E-twenty six)/ISRE (interferon-stimulated-response-element)-consensus element (EICE) in cluster E11 (AUC, 0.66; $p = 1.87 \times 10^{-45}$), rather than a peak-centered κB motif. EICE

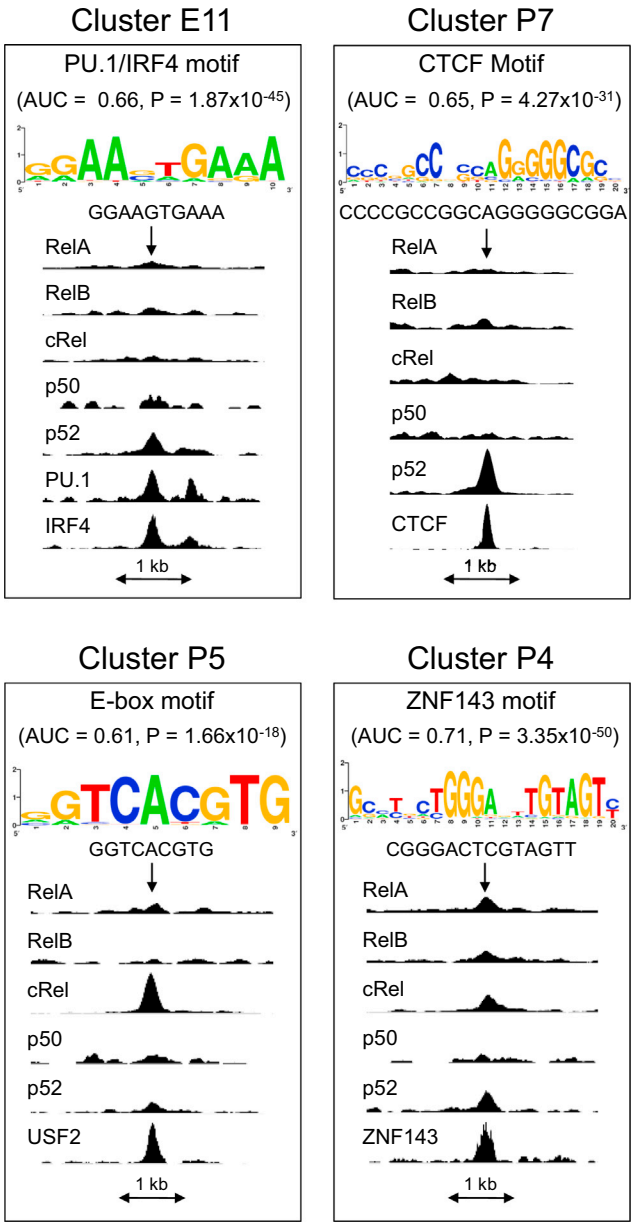

Figure 4. Alternative Motifs Enriched in Clusters that Lack κB Sites
De novo motif discovery revealed enrichment for E box, CTCF, composite PU.1/IRF4, and ZNF143 motifs at several clusters with low κB site enrichment. The discovered motif, AUC, and p value motif enrichment values, and ChIP-seq signals at representative loci, are shown.

motifs recruit PU.1 and IRF4 heterodimers and are essential for lymphocyte development and activation (Ochiai et al., 2013). Indeed, ENCODE GM12878 data confirmed PU.1 and IRF4 co-occupancy at many E11 sites (Figure 4). PU.1 may also function as a pioneer factor at these sites by creating areas of nucleosome-free DNA that are accessible to p52 (Ghisletti et al., 2010; Heinz et al., 2010; Smale, 2011). However, selective p52 recruitment to EICE sites, in the absence of enrichment for a κB motif or other identifiable motifs, is consistent with a direct role for PU.1 and IRF4 in p52 recruitment. Notably, PU.1 motifs were not identified as being enriched by de novo analysis in other clusters that lacked κB motif enrichment. p52 recruitment to EICE sites may thereby enable crosstalk between the noncanonical NF-κB, PU.1 and IRF4 pathways, each of which is important for B cell development and activation (Ochiai et al., 2013).

An alternative mechanism may selectively recruit p52 to P7 promoters, in the absence of κB motifs. De novo analysis instead identified the CTCF motif to be enriched within P7 ChIP-seq peaks (AUC, 0.65; $p = 4.27 \times 10^{-31}$), whereas the EICE motif was not significantly enriched in P7 (AUC, 0.52) (Figure 4). In support of a possible CTCF-dependent recruitment mechanism, ENCODE data demonstrated CTCF occupancy at many P7 sites (Figure 5). Because CTCF coordinates long-range interactions between DNA regulatory elements together with cohesin (Merkenschlager and Odom, 2013), we examined whether other cohesin complex members co-occupied P7 sites. Interestingly, 13.7% of P7 sites were co-occupied by SMC3 and RAD21, and 24.7% of P7 peaks were co-occupied by either SMC3 or RAD21 (Figures 5). Interestingly, long-range enhancer-promoter-looping interactions are used in RelA responses to tumor necrosis factor α (TNF-α) stimulation in human fibroblasts (Jin et al., 2013).

All NF-κB subunits except p50 were recruited to cluster P4 promoters, which were enriched for the ZNF143 motif (AUC, 0.71; $p = 3.35 \times 10^{-50}$). High ZNF143 ChIP signals were detected near the centers of cluster P4 promoters (Figures 4 and 5). How NF-κB is selectively recruited by ZNF143 to P4 promoters, but not other promoters bound by ZNF143, requires further investigation. Collectively, our data suggest that NF-κB recruitment to DNA in the absence of κB motifs significantly expands the range of NF-κB genomic targets and enables subunits to perform unique functions.

NF-κB-Predominant versus Highly Co-occupied LCL Sites

Comparison of our data sets with ENCODE ChIP-seq data, obtained for 65 other TFs in GM12878 cells, identified 2 classes of NF-κB-occupied promoters and enhancers. One class was bound either exclusively by NF-κB (clusters E4 and E7–E9) or by NF-κB in combination with a small number of other TFs (clusters E3, E10, P3, P6, and P8–P10) (Figure 5). The second class was bound by NF-κB together with many TFs, which occurred in different combinations across the cluster (clusters E1–E2, E5–E6, E11, P1–P5, and P7). Distinct TF profiles were generally apparent at enhancers versus promoter clusters (Figure 5).

NF-κB and FOXM1 Are Present Together in DNA-Bound Complexes at κB Sites

Incorporation of ENCODE GM12878 ChIP-seq data revealed that multiple TFs co-occurred with NF-κB, including both well-characterized and novel putative NF-κB cofactors. The oncogenic forkhead box TF FOXM1 was present at nearly 59% of enhancers occupied by NF-κB and at 50% of all NF-κB-occupied LCL sites. NF-κB co-occupied sites comprised nearly half of FOXM1 genome-wide binding in LCLs. Intriguingly, a κB motif, but not a forkhead recognition motif, was enriched at these sites (Figure 6A). At strong enhancers, as defined by chromatin states

Figure 5. Co-occurrence of NF-κB Subunits and GM12878 TF ChIP-Seq Peaks across Enhancer and Promoter Clusters

Red intensity indicates the extent of NF-κB co-occupancy with indicated TFs in GM12878 at promoter and enhancer clusters, normalized for the number of cluster elements and the number of total peaks for each TF. Basal TF names are indicated in green; DNA-looping factors are in blue.

(Ernst et al., 2011), FOXM1 and NF-κB subunit ChIP peak summit heights were correlated (Spearman R, 0.5 for p52). Moreover, FOXM1 co-occupied κB sites at many well-established NF-κB target genes, such as *TNFAIP3* (which encodes A20), *NFKBIA* (which encodes IκBα), *BIRC3* (which encodes cIAP2), and *CXCR4* (which encodes CXCR4) (Figures 6B and S4). These results suggest that NF-κB, or another factor that interacts with NF-κB, recruited FOXM1 to these LCL sites, particularly in clusters E1, E2, E5, E6, and E11.

NF-κB and FOXM1 are hyperactivated in many of the same malignancies (Ben-Neriah and Karin, 2011; Halasi and Gartel, 2013). Despite also having numerous overlapping biological roles, FOXM1 and NF-κB are not known to be cofactors. We therefore assessed whether FOXM1 and NF-κB were present together in DNA-bound protein complexes in LCLs. First, we used sequential GM12878 ChIP (ChIP re-ChIP), in which anti-FOXM1 ChIP was followed by ChIP using anti-RelA antibody, anti-FOXM1 antibody (positive control), or no antibody (negative control). Quantitative real-time PCR data showed that *PLK1* or *BCL2* target loci were significantly enriched in the RelA ChIP versus the control (Figure 6C), suggesting that NF-κB and FOXM1 are part of a DNA-bound protein complex. Second, electrophoretic mobility shift assays (EMSAs) using GM12878 nuclear extract and DNA probes representing the *PLK1* and *AURKA* regions further validated FOXM1 recruitment to κB sites. Supershift assays, in which antibodies against p50 or FOXM1 were added to the binding reaction, produced a slower migrating band, consistent with recruitment of both NF-κB and FOXM1 to the probe (Figure 6D). Notably, the probe contained a central κB site, but not a forkhead recognition motif, and had minimal flanking DNA, supporting FOXM1 recruitment by an NF-κB-dependent mechanism. A DNA probe with mutant κB site failed to compete for binding (Figure 6E). Finally, induced expression of a nondegradable IκBα superrepressor in IB4 LCLs significantly reduced both RelA and FOXM1 occupancy at the *PLK1* and *AURKA* loci (Figure 6F). Our results suggest that NF-κB and FOXM1 are present together in DNA-bound complexes at NF-κB sites and that recruitment to NF-κB sites is dependent on NF-κB DNA binding.

To investigate the functional consequences of FOXM1 recruitment to κB sites, we tested the effects of FOXM1 depletion on NF-κB target gene expression. By 48 hr after small hairpin RNA (shRNA) lentiviral delivery, each of three different anti-FOXM1 shRNAs strongly reduced FOXM1 expression and also markedly impaired expression of loci co-occupied by NF-κB and FOXM1, including *TNFAIP3*, *BIRC3*, *CXCR4*, *NFKBIA*, and *MAP3K7* (Figure 7A). By contrast, FOXM1 depletion did not impair expression of control LCL target genes, whose promoters and proximal enhancers were not occupied by either NF-κB or FOXM1 (Figure 7B). FOXM1 depletion did not affect cell viability at 48 hr posttransduction (Figures 7C and S5A). However, all three FOXM1 shRNAs reduced the number of cells in S phase and triggered apoptosis at 120 hr posttransduction (Figures 7D and S5B–S5D). Although NF-κB-independent FOXM1 cell-cycle roles may have strongly contributed to this phenotype, it nonetheless underscores FOXM1 as a novel LCL synthetic lethal target.

FOXM1 is a master regulator of germinal center B cell proliferation (Lefebvre et al., 2010) and is expressed in diffuse large B

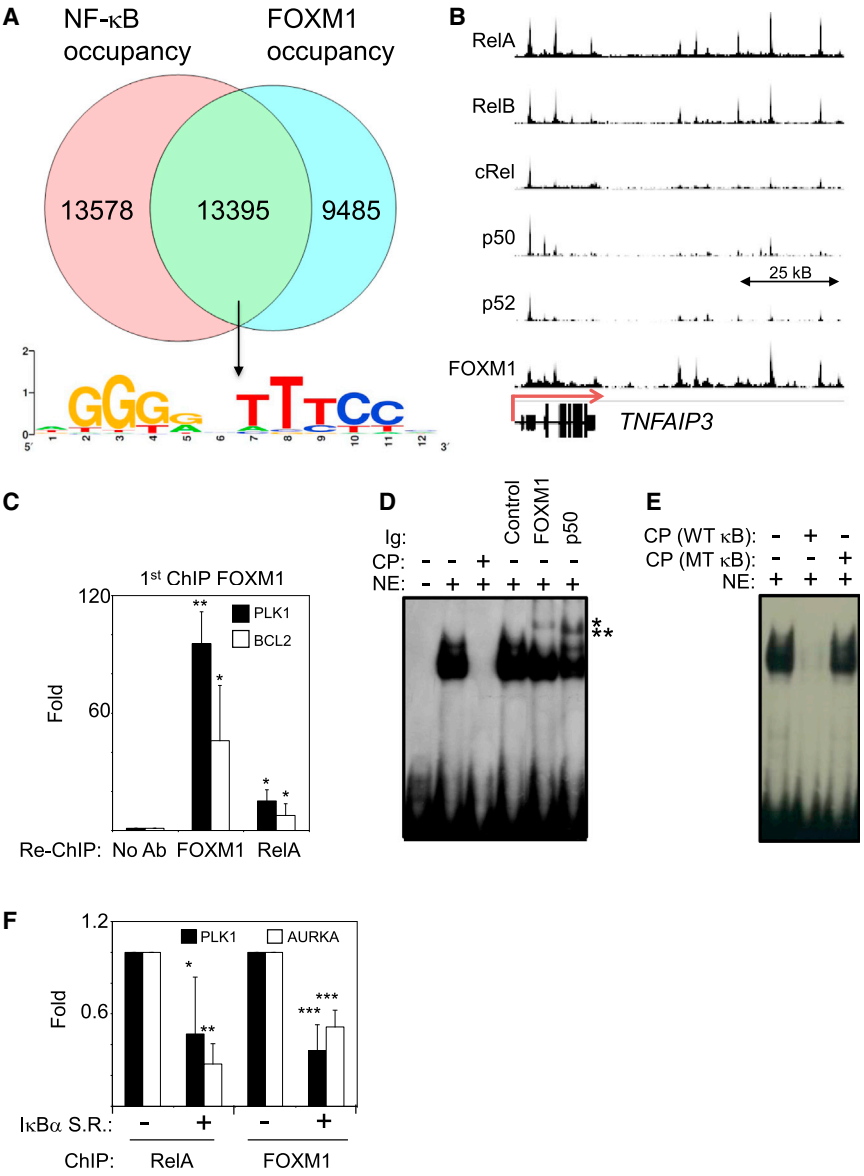

Figure 6. NF-κB and FOXM1 Are Present in DNA-Bound Protein Complexes at κB Sites

(A) Venn diagram showing the extent to which NF-κB and FOXM1 ChIP-seq peaks overlap in GM12878. The number of sites occupied by NF-κB, FOXM1, or co-occupied by both, and the consensus de novo motif for sites co-occupied by NF-κB and FOXM1, is shown.

(B) FOXM1 ChIP-seq signals at the *TNFAIP3* locus show a high degree of co-occupancy with NF-κB. See also Figure S4.

(C) ChIP-re-ChIP identified FOXM1 and RelA as present together in DNA-bound protein complexes at the *PLK1* and *BCL2* loci. FOXM1 ChIP was followed by RelA ChIP. Mean fold enrichment ± SD for replica experiments is shown. *$p < 0.05$; **$p < 0.01$.

(D) EMSA identified that both FOXM1 and NF-κB from GM12878 LCL nuclear extract (NE) bind a *PLK1* promoter DNA probe that contains a κB site, but no forkhead recognition site. Incubation with a cold probe (CP) is indicated. The single asterisk (*) indicates FOXM1 supershift. The double asterisks (**) indicate p50 supershifted band. A representative EMSA of three independent experiments is shown. Ig, immunoglobulin.

(E) A *PLK1* promoter probe with a central κB motif (wild-type [WT] κB), but not a probe with a mutant κB (MT κB) motif, competed for binding in EMSA (see Supplemental Experimental Procedures for full details).

(F) Inducible expression of an IκBα superrepressor (IκBα S.R.) in IB4 LCLs diminished RelA and FOXM1 ChIP signals at the *PLK1* and *AURKA* promoters. Mean + SD for replica experiments is shown. *$p < 0.05$; **$p < 0.01$; ***$p < 0.001$.

cell lymphoma (DLBCL) (Tompkins et al., 2013; Uddin et al., 2012). Impelled by these and our results, we investigated whether FOXM1 expression correlates with clinical outcome in DLBCL. We retrospectively analyzed microarray data sets from 414 DLBCL tumor samples (Lenz et al., 2008) and found that elevated FOXM1 expression levels were significantly correlated with worse overall survival, even controlling for tumor stage and subtype ($p = 0.0037$) (Figure 7E). Although FOXM1 roles independent of NF-κB may underlie this observation, our analysis nonetheless suggests that FOXM1 levels may be a valuable prognostic indicator in DLBCL.

DISCUSSION

In the classical model of NF-κB activation, stimuli trigger IκB degradation, NF-κB dimer nuclear translocation, and κB site binding. However, this model does not adequately consider the complexities that further shape NF-κB nuclear function (Oeckinghaus et al., 2011; Sen and Smale, 2010; Wan and Lenardo, 2010). Likewise, most genomic studies of NF-κB binding have focused on immediate events following canonical pathway stimulation by TNF-α or LPS and have not fully addressed why both pathways are needed to activate particular target genes. Our results provide a genomic survey of NF-κB subunit binding when both the canonical and noncanonical NF-κB signaling pathways are persistently active. Consequently, insights into the extent of crosstalk between the canonical and noncanonical pathways emerged.

The NF-κB-binding landscape in LCLs was complex, but largely describable in terms of a small number of SBPs, suggestive of both common and unique NF-κB subunit roles. Frequently, subunits activated by both the canonical and noncanonical pathways each contributed to SBPs. These results provide insights into how NF-κB may function during physiologic B cell activation, where CD40-mediated persistent activation of both the canonical and noncanonical pathways is central to the generation of germinal centers and humoral immunity (Kaileh

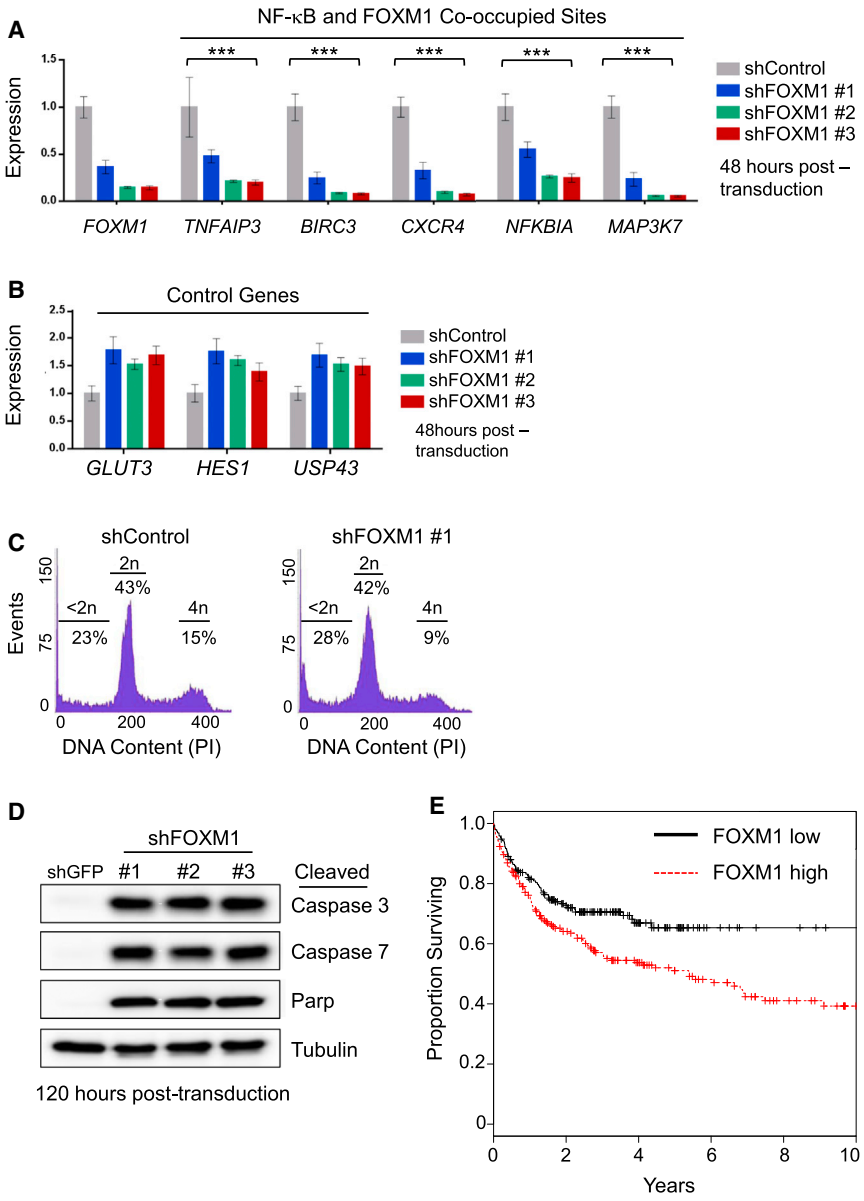

Figure 7. FOXM1 Cooperates with NF-κB to Regulate GM12878 Target Gene Expression

(A) Three independent shRNAs against FOXM1 reduced expression of key NF-κB target gene mRNAs by 48 hr after delivery. Mean ± SEM effects from three independent experiments are shown. $p < 0.05$ for TNFAIP3; $p < 0.01$ for all other comparisons between control and FOXM1 shRNAs. ***$p < 0.001$.

(B) FOXM1 shRNAs did not reduce expression control genes (which were not identified as NF-κB or FOXM1 targets in GM12878) at 48 hr post-shRNA delivery.

(C) FOXM1 depletion inhibited LCL proliferation and caused accumulation of subdiploid cells (<2n DNA content) by propidium iodide (PI) analysis. See also Figure S5.

(D) At 120 hr after shRNA delivery, FOXM1 depletion triggered cleavage of caspases 3 and 7 and their substrate, poly (ADP-ribose) polymerase (PARP). Tubulin load control is shown. Representative western blot of three independent experiments is shown.

(E) FOXM1 expression in DLBCL tumor samples correlated with worse clinical outcome. Retrospective analysis is shown of FOXM1 expression in microarray data sets obtained from 414 DLBCL tumor samples, and its relationship with patient survival. Wald test, $p = 0.0037$.

and Sen, 2012; Zarnegar et al., 2004). Our data sets provide a resource for studies of EBV oncoprotein-mediated NF-κB activation, constitutive NF-κB activity in tumors, and comparative genomics because many TF families similarly evolved by gene duplication and diversification.

Numerous NF-κB cofactors, for which GM12878 data are not yet available, might contribute to SBP formation. For instance, ENCODE ChIP-seq data are not yet available for RPS3, which binds to RelA and promotes RelA:p50 and RelA:RelA dimer binding to select κB sites (Wan and Lenardo, 2010). An important future area of investigation will be the identification of B cell cofactors that may similarly affect dimer-binding properties and thereby contribute to shaping the observed SBPs.

The extent to which NF-κB binding activates transcription remains an open question. Studies in TNF-α-stimulated LCLs and LPS-stimulated THP-1 monocytes suggested that only a minority of RelA-binding events induce transcription (Lim et al., 2007; Martone et al., 2003). However, limitations in the assignment of enhancers to their target genes may have resulted in underestimates of regulatory binding events. In contrast, we found that nearly all NF-κB binding in LCLs, including by p50 and p52, occurred at highly active enhancers or promoters. Indeed, NF-κB promoter occupancy highly correlates with induction of transcription in LPS-stimulated monocytes (Schreiber et al., 2006), and the vast majority of NF-κB-binding events occur at active promoters and enhancers in LPS-stimulated murine dendritic cells (Garber et al., 2012).

Nearly one-third of LCL NF-κB-binding events occurred at DNA sites lacking κB motifs. cRel and p52 may more frequently be recruited to these sites (clusters P5, P7, E10, and E11). Consistent with our findings, a prior ChIP-ChIP study of RelA chromosome 22-binding events in TNF-α-stimulated HeLa cells reported that 44% of identified RelA sites did not have a κB motif (Martone et al., 2003). Similarly, ChIP-paired-end tag analysis of LPS-stimulated THP-1 cells found the RelA motif to be absent at 57% of RelA-binding sites (Lim et al., 2007). However, alternative NF-κB recruitment motifs were not identified. We report four motifs that are highly enriched at LCL NF-κB-binding sites that lack κB motifs: E boxes at cRel-occupied promoters, ZNF143 motifs at promoters occupied by all NF-κB subunits except p50, CTCF

sites at p52-occupied promoters, and ETS/ISRE elements at p52-occupied enhancers. Indirect recruitment to sites lacking κB motifs may provide an important mechanism through which NF-κB subunits perform specific functions and crosstalk with other pathways. Our analysis offers insights into why each NF-κB subunit has nonredundant roles in B cells (Gerondakis et al., 2006).

NF-κB requires additional transcription cofactors to fully activate target gene expression (Natoli et al., 2005; Oeckinghaus et al., 2011; Wan and Lenardo, 2010). Certain promoter and enhancer clusters were co-occupied by at least ten additional TFs, though it is likely that fewer bind to an individual site at the same time. Binding at these loci is unlikely to be an artifact of the ChIP experimental procedures because SBPs with the highest co-occupancy (e.g., P1, E1, and E2) were enriched for κB-binding site sequences. NF-κB was also found to bind frequently at highly co-occupied sites in LPS-stimulated murine dendritic cells (Garber et al., 2012). High TF co-occupancy may be due to a more accessible chromatin state at these genomic regions (Figure S7).

Our data highlight FOXM1 as an important coactivator of NF-κB target gene transcription in LCLs, present at 50% of all NF-κB peaks. Because a FOXM1 DNA motif was not enriched at these sites, our data are consistent with a model in which NF-κB recruits FOXM1 to κB sites, either directly or indirectly, through additional cofactors. In support of the former possibility, the MMB activator complex directly recruits FOXM1 to coactivate transcription (Chen et al., 2013). MuvB and B-Myb also interact with FOXM1 to regulate gene expression during the G2 phase of cell cycle (Sadasivam et al., 2012). Curiously, we did not find evidence for NF-κB recruitment to FOXM1-bound forkhead box recognition sites; DNA allostery may induce conformation changes in the bound TF, leading to differences in protein-protein interactions (Leung et al., 2004). FOXM1 depletion impaired transcription of key NF-κB target genes and ultimately induced LCL apoptosis, reminiscent of the phenotype of NF-κB inhibition on these cells (Cahir-McFarland et al., 2000).

To our knowledge, FOXM1 has not previously been reported to function jointly with NF-κB in target gene regulation. However, crosstalk between NF-κB and FOXM1 may underlie published studies. Both FOXM1 and NF-κB are implicated in the pathogenesis of K-Ras-induced non-small-cell lung cancer (Wang et al., 2013). Moreover, conditional FOXM1 deletion impairs K-Ras-mediated expression of multiple NF-κB pathway components, including IKK-β, RelA, p105/p50, and p100/p52. Intriguingly, NF-κB and FOXM1 have each been implicated as drivers of B cell lymphomagenesis (Green et al., 2011; Lim et al., 2012; Tompkins et al., 2013; Uddin et al., 2012), although a joint role of FOXM1 and NF-κB in driving B cell malignancy has not yet been proposed.

Despite the promise of therapies that block pathogenic NF-κB hyperactivity in cancer and autoimmune diseases, side effects have largely precluded the use of broadly acting NF-κB inhibitors, such as IKK-β kinase antagonists. Uncovering subunit-specific transcriptional mechanisms may facilitate approaches to selectively alter NF-κB target gene expression. Targets that require both canonical and noncanonical NF-κB pathway activation may be particularly sensitive to disruption. Because FOXM1 is not expressed in most adult tissues, our data highlight the FOXM1 pathway as a potential therapeutic target in B cell malignancy. An increasingly sophisticated understanding of NF-κB nuclear function promises to highlight novel therapeutic strategies for selective NF-κB inhibition.

EXPERIMENTAL PROCEDURES

Cell Lines and Antibodies

GM12878 and IB4 cells expressing tetracycline-regulated IκBα superrepressor (Cahir-McFarland et al., 2000) were used. Antibodies used are in the Supplemental Experimental Procedures.

ChIP-Seq and Peak Calling

GM12878 ChIP-seq was done as described (Zhao et al., 2011). See Supplemental Experimental Procedures for full details.

We used SPP v.1.10 (Kharchenko et al., 2008) to identify regions with high enrichment of ChIP-seq tags ("peaks"). We used the IDR framework to determine statistically significant peaks. For each subunit, we directly compared the peaks obtained in replicate experiments and set the peak calling threshold to yield an IDR of 1%.

Chromatin State Distribution

GM12878 ChromHMM chromatin state annotations (Ernst et al., 2011) were used.

Comparison with ENCODE ChIP-Seq Data

We computed the fraction of NF-κB peak regions that overlapped with ENCODE ChIP-seq peaks for all available experiments. Co-occurrence scores were normalized for peak width and height, the number of total peaks in each experiment, and the number of peaks included in each cluster.

De Novo Motif Discovery

We employed ChIPMunk (Kulakovskiy et al., 2010) and the MEME-ChIP suite (Bailey et al., 2009) to discover potential regulatory motifs in the NF-κB and ENCODE ChIP-seq data. The discovered de novo motifs were compared with existing motifs using the dictionary of vertebrate motifs in HOMER v.3.0 (Heinz et al., 2010).

Motif Enrichment Determination

We used the AUC statistic to quantify motif enrichment. See also Supplemental Experimental Procedures.

Gene Set Enrichment and Evolutionary Conservation Analysis

We used GREAT to predict potential biological functions of different clusters of NF-κB ChIP-seq-bound regions and the Genomic Evolutionary Rate Profiling++ (GERP++) score, calculated over an evolutionary tree of 33 mammals, as a measure of evolutionary constraint in the human genome. Full details are in Supplemental Experimental Procedures.

Analysis of DLBCL Data Sets

We used a Cox proportional hazards model to determine whether FOXM1 expression was predictive of survival in patients with DLBCL. The p value was calculated by performing a Wald test on the FOXM1 expression coefficient after fitting the model to the data, controlling for tumor stage and the microarray-derived diagnosis as part of the model.

ChIP, ChIP-Re-ChIP, and Quantitative PCR

ChIP assays were performed with the indicated antibodies. Quantitative PCR was used to quantify NF-κB binding to indicated sites. Re-ChIP-IT kit (Active Motif) was used for ChIP-re-ChIP experiments following the manufacturer's protocol.

Cell Cycle and Apoptosis Assays

Lentivirus-transduced GM12878 cells were selected with puromycin, fixed with 70% ethanol, stained with propidium iodide, and analyzed by

fluorescence-activated cell sorting. Caspase activity was determined using Caspase-Glo assay or by western blot.

ACCESSION NUMBERS

The GEO accession number for the NF-κB ChIP-seq data reported in this paper is GSE55105.

SUPPLEMENTAL INFORMATION

Supplemental Information includes Supplemental Experimental Procedures, seven figures, and two tables and can be found with this article online at http://dx.doi.org/10.1016/j.celrep.2014.07.037.

AUTHOR CONTRIBUTIONS

B.Z., L.A.B., E.C.-M., E.K., and B.E.G. designed the study. B.Z., M.K., M.L.B., E.K., and B.E.G. supervised research. B.Z., I.E., B.W., S.C.S.S., T.T.S., H.G., S.B.M., K.T., and B.E.G. performed experiments. L.A.B. performed the computational data analysis. L.A.B., B.Z., B.E.G., E.K, and M.L.B. analyzed data. L.A.B., B.Z., and B.E.G. wrote the Supplemental Experimental Procedures. B.Z., S.J., and H.Z. provided analytic tools. L.A.B., B.Z., and B.E.G. prepared figures and/or tables. B.E.G., L.A.B., B.Z., E.K., and M.L.B. wrote the manuscript.

ACKNOWLEDGMENTS

This project was supported by a Burroughs Wellcome Medical Scientist career award (to B.E.G.), NIH K08 CA140780 (to B.E.G.), NIH RO1 CA085180, CA170023, and CA047006 (to E.K.), a National Science Foundation Graduate Research Fellowship (to L.A.B.), and grant R01 HG003985 from NIH/NHGRI (to M.L.B.). We thank Trevor Siggers and Suzanne Gaudet for critical reading of the manuscript.

Received: March 4, 2014
Revised: June 9, 2014
Accepted: July 21, 2014
Published: August 21, 2014

REFERENCES

Baek, S.H., Ohgi, K.A., Rose, D.W., Koo, E.H., Glass, C.K., and Rosenfeld, M.G. (2002). Exchange of N-CoR corepressor and Tip60 coactivator complexes links gene expression by NF-kappaB and beta-amyloid precursor protein. Cell *110*, 55–67.

Bailey, T.L., Boden, M., Buske, F.A., Frith, M., Grant, C.E., Clementi, L., Ren, J., Li, W.W., and Noble, W.S. (2009). MEME SUITE: tools for motif discovery and searching. Nucleic Acids Res. *37*, W202–W208.

Ben-Neriah, Y., and Karin, M. (2011). Inflammation meets cancer, with NF-κB as the matchmaker. Nat. Immunol. *12*, 715–723.

Bonizzi, G., and Karin, M. (2004). The two NF-kappaB activation pathways and their role in innate and adaptive immunity. Trends Immunol. *25*, 280–288.

Cahir-McFarland, E.D., Davidson, D.M., Schauer, S.L., Duong, J., and Kieff, E. (2000). NF-kappa B inhibition causes spontaneous apoptosis in Epstein-Barr virus-transformed lymphoblastoid cells. Proc. Natl. Acad. Sci. USA *97*, 6055–6060.

Chen, F.E., and Ghosh, G. (1999). Regulation of DNA binding by Rel/NF-kappaB transcription factors: structural views. Oncogene *18*, 6845–6852.

Chen, X., Müller, G.A., Quaas, M., Fischer, M., Han, N., Stutchbury, B., Sharrocks, A.D., and Engeland, K. (2013). The forkhead transcription factor FOXM1 controls cell cycle-dependent gene expression through an atypical chromatin binding mechanism. Mol. Cell. Biol. *33*, 227–236.

Ernst, J., Kheradpour, P., Mikkelsen, T.S., Shoresh, N., Ward, L.D., Epstein, C.B., Zhang, X., Wang, L., Issner, R., Coyne, M., et al. (2011). Mapping and analysis of chromatin state dynamics in nine human cell types. Nature *473*, 43–49.

Garber, M., Yosef, N., Goren, A., Raychowdhury, R., Thielke, A., Guttman, M., Robinson, J., Minie, B., Chevrier, N., Itzhaki, Z., et al. (2012). A high-throughput chromatin immunoprecipitation approach reveals principles of dynamic gene regulation in mammals. Mol. Cell *47*, 810–822.

Gerondakis, S., Grumont, R., Gugasyan, R., Wong, L., Isomura, I., Ho, W., and Banerjee, A. (2006). Unravelling the complexities of the NF-kappaB signalling pathway using mouse knockout and transgenic models. Oncogene *25*, 6781–6799.

Ghisletti, S., Barozzi, I., Mietton, F., Polletti, S., De Santa, F., Venturini, E., Gregory, L., Lonie, L., Chew, A., Wei, C.L., et al. (2010). Identification and characterization of enhancers controlling the inflammatory gene expression program in macrophages. Immunity *32*, 317–328.

Green, M.R., Aya-Bonilla, C., Gandhi, M.K., Lea, R.A., Wellwood, J., Wood, P., Marlton, P., and Griffiths, L.R. (2011). Integrative genomic profiling reveals conserved genetic mechanisms for tumorigenesis in common entities of non-Hodgkin's lymphoma. Genes Chromosomes Cancer *50*, 313–326.

Halasi, M., and Gartel, A.L. (2013). FOX(M1) news—it is cancer. Mol. Cancer Ther. *12*, 245–254.

Hayden, M.S., and Ghosh, S. (2012). NF-κB, the first quarter-century: remarkable progress and outstanding questions. Genes Dev. *26*, 203–234.

Heinz, S., Benner, C., Spann, N., Bertolino, E., Lin, Y.C., Laslo, P., Cheng, J.X., Murre, C., Singh, H., and Glass, C.K. (2010). Simple combinations of lineage-determining transcription factors prime cis-regulatory elements required for macrophage and B cell identities. Mol. Cell *38*, 576–589.

Heinz, S., Romanoski, C.E., Benner, C., Allison, K.A., Kaikkonen, M.U., Orozco, L.D., and Glass, C.K. (2013). Effect of natural genetic variation on enhancer selection and function. Nature *503*, 487–492.

Huang, T.T., Kudo, N., Yoshida, M., and Miyamoto, S. (2000). A nuclear export signal in the N-terminal regulatory domain of IkappaBalpha controls cytoplasmic localization of inactive NF-kappaB/IkappaBalpha complexes. Proc. Natl. Acad. Sci. USA *97*, 1014–1019.

Jin, F., Li, Y., Dixon, J.R., Selvaraj, S., Ye, Z., Lee, A.Y., Yen, C.A., Schmitt, A.D., Espinoza, C.A., and Ren, B. (2013). A high-resolution map of the three-dimensional chromatin interactome in human cells. Nature *503*, 290–294.

Kaileh, M., and Sen, R. (2012). NF-κB function in B lymphocytes. Immunol. Rev. *246*, 254–271.

Kasowski, M., Grubert, F., Heffelfinger, C., Hariharan, M., Asabere, A., Waszak, S.M., Habegger, L., Rozowsky, J., Shi, M., Urban, A.E., et al. (2010). Variation in transcription factor binding among humans. Science *328*, 232–235.

Kharchenko, P.V., Tolstorukov, M.Y., and Park, P.J. (2008). Design and analysis of ChIP-seq experiments for DNA-binding proteins. Nat. Biotechnol. *26*, 1351–1359.

Kulakovskiy, I.V., Boeva, V.A., Favorov, A.V., and Makeev, V.J. (2010). Deep and wide digging for binding motifs in ChIP-Seq data. Bioinformatics *26*, 2622–2623.

Landt, S.G., Marinov, G.K., Kundaje, A., Kheradpour, P., Pauli, F., Batzoglou, S., Bernstein, B.E., Bickel, P., Brown, J.B., Cayting, P., et al. (2012). ChIP-seq guidelines and practices of the ENCODE and modENCODE consortia. Genome Res. *22*, 1813–1831.

Lefebvre, C., Rajbhandari, P., Alvarez, M.J., Bandaru, P., Lim, W.K., Sato, M., Wang, K., Sumazin, P., Kustagi, M., Bisikirska, B.C., et al. (2010). A human B-cell interactome identifies MYB and FOXM1 as master regulators of proliferation in germinal centers. Mol. Syst. Biol. *6*, 377.

Lenz, G., Wright, G., Dave, S.S., Xiao, W., Powell, J., Zhao, H., Xu, W., Tan, B., Goldschmidt, N., Iqbal, J., et al.; Lymphoma/Leukemia Molecular Profiling Project (2008). Stromal gene signatures in large-B-cell lymphomas. N. Engl. J. Med. *359*, 2313–2323.

Leung, T.H., Hoffmann, A., and Baltimore, D. (2004). One nucleotide in a kappaB site can determine cofactor specificity for NF-kappaB dimers. Cell *118*, 453–464.

Lim, C.A., Yao, F., Wong, J.J., George, J., Xu, H., Chiu, K.P., Sung, W.K., Lipovich, L., Vega, V.B., Chen, J., et al. (2007). Genome-wide mapping of RELA(p65) binding identifies E2F1 as a transcriptional activator recruited by NF-kappaB upon TLR4 activation. Mol. Cell *27*, 622–635.

Lim, K.H., Yang, Y., and Staudt, L.M. (2012). Pathogenetic importance and therapeutic implications of NF-κB in lymphoid malignancies. Immunol. Rev. *246*, 359–378.

Liu, J., and Beller, D.I. (2003). Distinct pathways for NF-kappa B regulation are associated with aberrant macrophage IL-12 production in lupus- and diabetes-prone mouse strains. J. Immunol. *170*, 4489–4496.

Longnecker, R., Kieff, E., and Cohen, J.I. (2013). Epstein-Barr Virus. In Fields Virology, D.M. Knipe and P.M. Howley, eds. (Philadelphia: Lippincott, Williams and Wilkins), pp. 1898–1959.

Martone, R., Euskirchen, G., Bertone, P., Hartman, S., Royce, T.E., Luscombe, N.M., Rinn, J.L., Nelson, F.K., Miller, P., Gerstein, M., et al. (2003). Distribution of NF-kappaB-binding sites across human chromosome 22. Proc. Natl. Acad. Sci. USA *100*, 12247–12252.

McLean, C.Y., Bristor, D., Hiller, M., Clarke, S.L., Schaar, B.T., Lowe, C.B., Wenger, A.M., and Bejerano, G. (2010). GREAT improves functional interpretation of cis-regulatory regions. Nat. Biotechnol. *28*, 495–501.

Merkenschlager, M., and Odom, D.T. (2013). CTCF and cohesin: linking gene regulatory elements with their targets. Cell *152*, 1285–1297.

Müller, C.W., Rey, F.A., Sodeoka, M., Verdine, G.L., and Harrison, S.C. (1995). Structure of the NF-kappa B p50 homodimer bound to DNA. Nature *373*, 311–317.

Natoli, G. (2009). Control of NF-kappaB-dependent transcriptional responses by chromatin organization. Cold Spring Harb. Perspect. Biol. *1*, a000224.

Natoli, G., Saccani, S., Bosisio, D., and Marazzi, I. (2005). Interactions of NF-kappaB with chromatin: the art of being at the right place at the right time. Nat. Immunol. *6*, 439–445.

Nissen, R.M., and Yamamoto, K.R. (2000). The glucocorticoid receptor inhibits NFkappaB by interfering with serine-2 phosphorylation of the RNA polymerase II carboxy-terminal domain. Genes Dev. *14*, 2314–2329.

Ochiai, K., Maienschein-Cline, M., Simonetti, G., Chen, J., Rosenthal, R., Brink, R., Chong, A.S., Klein, U., Dinner, A.R., Singh, H., and Sciammas, R. (2013). Transcriptional regulation of germinal center B and plasma cell fates by dynamical control of IRF4. Immunity *38*, 918–929.

Oeckinghaus, A., Hayden, M.S., and Ghosh, S. (2011). Crosstalk in NF-κB signaling pathways. Nat. Immunol. *12*, 695–708.

Rahman, M.M., and McFadden, G. (2011). Modulation of NF-κB signalling by microbial pathogens. Nat. Rev. Microbiol. *9*, 291–306.

Rodriguez, M.S., Thompson, J., Hay, R.T., and Dargemont, C. (1999). Nuclear retention of IkappaBalpha protects it from signal-induced degradation and inhibits nuclear factor kappaB transcriptional activation. J. Biol. Chem. *274*, 9108–9115.

Saccani, S., Pantano, S., and Natoli, G. (2003). Modulation of NF-kappaB activity by exchange of dimers. Mol. Cell *11*, 1563–1574.

Sadasivam, S., Duan, S., and DeCaprio, J.A. (2012). The MuvB complex sequentially recruits B-Myb and FoxM1 to promote mitotic gene expression. Genes Dev. *26*, 474–489.

Schreiber, J., Jenner, R.G., Murray, H.L., Gerber, G.K., Gifford, D.K., and Young, R.A. (2006). Coordinated binding of NF-kappaB family members in the response of human cells to lipopolysaccharide. Proc. Natl. Acad. Sci. USA *103*, 5899–5904.

Sen, R., and Smale, S.T. (2010). Selectivity of the NF-κB response. Cold Spring Harb. Perspect. Biol. *2*, a000257.

Shih, V.F., Tsui, R., Caldwell, A., and Hoffmann, A. (2011). A single NFκB system for both canonical and non-canonical signaling. Cell Res. *21*, 86–102.

Siggers, T., Chang, A.B., Teixeira, A., Wong, D., Williams, K.J., Ahmed, B., Ragoussis, J., Udalova, I.A., Smale, S.T., and Bulyk, M.L. (2012). Principles of dimer-specific gene regulation revealed by a comprehensive characterization of NF-κB family DNA binding. Nat. Immunol. *13*, 95–102.

Smale, S.T. (2011). Hierarchies of NF-κB target-gene regulation. Nat. Immunol. *12*, 689–694.

Sun, S.C. (2011). Non-canonical NF-κB signaling pathway. Cell Res. *21*, 71–85.

Tompkins, V.S., Han, S.S., Olivier, A., Syrbu, S., Bair, T., Button, A., Jacobus, L., Wang, Z., Lifton, S., Raychaudhuri, P., et al. (2013). Identification of candidate B-lymphoma genes by cross-species gene expression profiling. PLoS One *8*, e76889.

Uddin, S., Hussain, A.R., Ahmed, M., Siddiqui, K., Al-Dayel, F., Bavi, P., and Al-Kuraya, K.S. (2012). Overexpression of FoxM1 offers a promising therapeutic target in diffuse large B-cell lymphoma. Haematologica *97*, 1092–1100.

Wan, F., and Lenardo, M.J. (2010). The nuclear signaling of NF-kappaB: current knowledge, new insights, and future perspectives. Cell Res. *20*, 24–33.

Wang, W., Tam, W.F., Hughes, C.C., Rath, S., and Sen, R. (1997). c-Rel is a target of pentoxifylline-mediated inhibition of T lymphocyte activation. Immunity *6*, 165–174.

Wang, I.C., Ustiyan, V., Zhang, Y., Cai, Y., Kalin, T.V., and Kalinichenko, V.V. (2013). Foxm1 transcription factor is required for the initiation of lung tumorigenesis by oncogenic Kras(G12D.). Oncogene, Published online November 11, 2013. http://dx.doi.org/10.1038/onc.2013.

Yamazaki, T., and Kurosaki, T. (2003). Contribution of BCAP to maintenance of mature B cells through c-Rel. Nat. Immunol. *4*, 780–786.

Ye, T., Krebs, A.R., Choukrallah, M.A., Keime, C., Plewniak, F., Davidson, I., and Tora, L. (2011). seqMINER: an integrated ChIP-seq data interpretation platform. Nucleic Acids Res. *39*, e35.

Zarnegar, B., He, J.Q., Oganesyan, G., Hoffmann, A., Baltimore, D., and Cheng, G. (2004). Unique CD40-mediated biological program in B cell activation requires both type 1 and type 2 NF-kappaB activation pathways. Proc. Natl. Acad. Sci. USA *101*, 8108–8113.

Zhao, B., Zou, J., Wang, H., Johannsen, E., Peng, C.W., Quackenbush, J., Mar, J.C., Morton, C.C., Freedman, M.L., Blacklow, S.C., et al. (2011). Epstein-Barr virus exploits intrinsic B-lymphocyte transcription programs to achieve immortal cell growth. Proc. Natl. Acad. Sci. USA *108*, 14902–14907.